PHYSICAL REVIEW B **84**, 020505(R) (2011)

Domain-wall and reverse-domain superconducting states of a Pb thin-film bridge on a ferromagnetic $BaFe_{12}O_{19}$ single crystal

R. Werner,[1] A. Yu. Aladyshkin,[2,3] S. Guénon,[1] J. Fritzsche,[2] I. M. Nefedov,[3] V. V. Moshchalkov,[2] R. Kleiner,[1] and D. Koelle[1,*]

[1]*Physikalisches Institut–Experimentalphysik II and Center for Collective Quantum Phenomena in LISA$^+$, Universität Tübingen, Auf der Morgenstelle 14, D-72076 Tübingen, Germany*

[2]*INPAC–Institute for Nanoscale Physics and Chemistry, K.U. Leuven, Celestijnenlaan 200D, B-3001 Leuven, Belgium*

[3]*Institute for Physics of Microstructures RAS, 603950 Nizhny Novgorod, GSP-105, Russia*

(Received 14 February 2011; revised manuscript received 13 May 2011; published 20 July 2011)

We report on imaging of the nonuniform superconducting states in a Pb thin-film bridge on top of a ferromagnetic $BaFe_{12}O_{19}$ single crystal with a single straight domain wall along the center of the bridge by low-temperature scanning laser microscopy. We have visualized domain-wall superconductivity (DWS) close to the critical temperature of Pb, when the Pb film above the domain wall acts as a superconducting path for the current. The evolution of the DWS signal with temperature and the external-field-driven transition from DWS to reverse-domain superconductivity was visualized.

DOI: 10.1103/PhysRevB.84.020505 PACS number(s): 74.78.Na, 74.25.Op, 75.47.−m

It is well known that so-called surface or bound states can be generated by the presence of boundaries in a material. For example, the formation of surface states for a single electron wave function in a semi-infinite crystalline lattice due to the modification of the boundary conditions was described by Tamm[1] and by Shockley.[2] Other examples of bound states are surface plasmons, propagating along the interface between a dielectric and a metal,[3–5] and surface acoustic waves traveling along the surface of a material exhibiting elasticity.[6,7] In both latter cases these waves are confined in the direction perpendicular to the wave vector, i.e., their amplitudes decay exponentially far from the interface or surface. The formation of surface bound states for the superconducting order-parameter wave function Ψ was considered by Saint-James and de Gennes.[8,9] They showed that localized superconductivity at a superconductor (S)/vacuum or S/insulator interface can appear at an applied magnetic field $H_{\rm ext}$ above the upper critical field H_{c2} for bulk superconductivity. Similarly to this surface superconductivity, localized superconductivity can also nucleate near the sample edge in a thin semi-infinite superconducting film[10] or in a thin superconducting disk of very large diameter[11] in a *perpendicular* magnetic field. Such so-called edge superconductivity (ES), with transition temperature $T_c^{\rm ES}$, has the same phase-transition line as surface superconductivity,[12] given by $1-T_c^{\rm ES}/T_{c0}\simeq 0.59\,|H_{\rm ext}|/H_{c2}^{(0)}$. Here, T_{c0} is the superconducting transition temperature in zero magnetic field, $H_{c2}^{(0)}=\Phi_0/(2\pi\xi_0^2)$ and ξ_0 are the upper critical field and coherence length at temperature $T=0$, respectively, and $\Phi_0=\pi\hbar c/e$ is the magnetic-flux quantum. This means that ES will survive up to the critical field $H_{c3}=1.69H_{c2}$, while above $H_{c2}=H_{c2}^{(0)}(1-T/T_{c0})$ bulk superconductivity is totally suppressed.

An alternative way to prepare localized states in superconducting films is to confine the order-parameter wave function by a nonuniform magnetic field in hybrid S/ferromagnet (F) structures (see, e.g., Ref. 13 and references therein). Buzdin and Mel'nikov[14] considered a steplike distribution $b_z(x)=B_0\,{\rm sgn}(x)$ of the perpendicular component of the magnetic field, $B_z=H_{\rm ext}+b_z$, induced by domain walls in the ferromagnet (with the z axis perpendicular to the film surface). They demonstrated that superconductivity will survive in vicinity along the step, even if the amplitude of the nonuniform magnetic $B_0>H_{c2}$. The dependence of the transition temperature $T_c^{\rm DWS}(H_{\rm ext})$ for *domain-wall superconductivity* (DWS) in a plain superconducting film (i.e., infinite in lateral direction) can be estimated as $1-T_c^{\rm DWS}/T_{c0}\simeq\{0.59-0.70(H_{\rm ext}/B_0)^2+0.09(H_{\rm ext}/B_0)^4\}B_0/H_{c2}^{(0)}$.[15]

For flux-coupled S/F structures of finite lateral size the localized states of ES and DWS may compete as illustrated in Fig. 1 for the case of a thin-film S strip of finite width above a F substrate with a domain wall along the center of the bridge, for $H_{c2}<B_0<H_{c3}$. For a domain structure with steplike $b_z(x)$ profile and $H_{\rm ext}=0$, ES and DWS nucleate simultaneously in the S strip as shown in Fig. 1(a). Figure 1(b) shows the case of a domain wall with finite width and $H_{\rm ext}=0$. Here, DWS becomes energetically more favorable compared to ES and only DWS nucleates.[16] For $H_{\rm ext}\neq 0$, the local field is compensated above the domain with magnetization direction opposite to $H_{\rm ext}$. If $||H_{\rm ext}|-B_0|<H_{c2}$ superconductivity is turned on above this reverse domain while it is still suppressed above the parallel domain [cf. Fig. 1(c)]. This effect is termed *reverse-domain superconductivity* (RDS).[17,18] We note that when H_{c2} becomes larger than $|H_{\rm ext}|+B_0$ (e.g., upon cooling) above the parallel domain, superconductivity may also nucleate there and the entire strip will be in the superconducting state, which we call *complete superconductivity* (CS).

Fingerprints of RDS and DWS have been found by electric transport measurements on S/F hybrids with a rather complex domain structure in $BaFe_{12}O_{19}$ (BFO) crystals[17] and multilayered CoPt films[19] with perpendicular magnetic anisotropy. Using low-temperature scanning laser microscopy (LTSLM), RDS has been visualized in a hybrid $Nb/PbFe_{12}O_{19}$ system.[18] However, due to the complex domain structure and relatively small domain size, visualization of DWS was not possible. Recently, significant improvements have been achieved, regarding the fabrication of specially polished BFO crystals, characterized by a well defined and stable domain structure with straight domain walls separated by typically 30 μm.[20,21] Here we report on the direct imaging of the development of DWS and RDS in a hybrid S/F

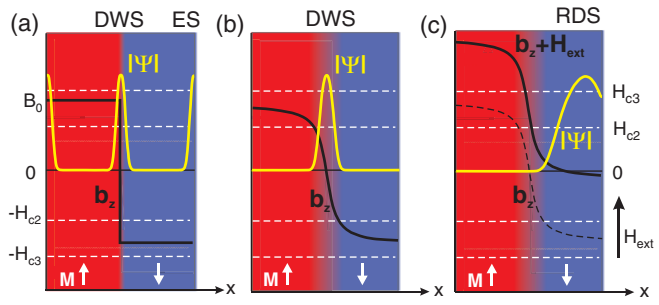

FIG. 1. (Color online) Illustration of DWS, ES, and RDS across a thin-film S strip on top of a F substrate with two domains with perpendicular magnetization $\boldsymbol{M}$. Magnetic-field profiles $B_z(x) = H_{\rm ext} + b_z(x)$ inside the S strip generated by the domains underneath and modulus of superconducting order parameter $|\Psi(x)|$ are shown for (a) steplike $b_z(x)$ for $H_{\rm ext} = 0$, (b) field profile with finite width for $H_{\rm ext} = 0$, and (c) finite $H_{\rm ext} \approx B_0$. White dashed lines indicate upper critical fields $\pm H_{c2}$ and $\pm H_{c3}$.

structure, consisting of a superconducting Pb film on top of a ferromagnetic BFO crystal by means of LTSLM.[18,22–25]

We prepared a 40-nm-thick and 30-μm-wide Pb microbridge on top of a BFO substrate, so that only a single domain wall is running along the center of the Pb bridge parallel to the current flow. The BFO substrate and the Pb thin film were separated by a 4-nm-thick insulating Ge layer so that the system is only flux coupled. From resistance R vs $H_{\rm ext}$ measurements at variable T of a reference sample with several domain walls oriented perpendicular to the long side of the bridge,[26] we compose the $H_{\rm ext}$-T phase diagram shown in Fig. 2(b).

For imaging by LTSLM, the sample was mounted on the cold finger of a helium gas flow cryostat, with an optical window to enable irradiation of the sample surface in the (x,y) plane by a focused laser beam with beam spot diameter $\sim$1.5–2 μm.[24,25] The amplitude modulated laser beam (at frequency $f \approx 10$ kHz) induces a local increase of temperature $\delta T(x - x_0, y - y_0)$ centered at the beam spot position (x_0, y_0) on the sample surface. During imaging, the Pb bridge is biased at a constant current I, and the beam-induced change of voltage $\Delta V(x_0, y_0)$ is recorded with lock-in technique. The LTSLM voltage signal can be interpreted as follows: If the irradiated part of the sample was in the normal state with resistivity ρ_n, the laser beam induces a very small voltage signal $\Delta V \propto \partial\rho_n/\partial T$. However, if the irradiated region took part in the transfer of a substantial part of the supercurrents, the beam-induced suppression of superconductivity might switch the sample from a low-resistive state to a high-resistive state. This effect should be maximal if I is close to the overall critical current $I_c = I_c(T, H_{\rm ext})$ of the sample. In this case LTSLM allows one to map out the ability of the sample to carry supercurrents.

In order to trace out the evolution of DWS with temperature, we recorded a series of LTSLM voltage images $\Delta V(x,y)$ at $H_{\rm ext} = 0$ and different T across the resistive transition of the Pb bridge. Figure 2(a) shows the $R(T)$ curve of the Pb/BFO microbridge; the labels 1–8 indicate the bias points for which LTSLM images and line scans are shown in Figs. 2(d) and 2(c), respectively. The dots in the $H_{\rm ext}$-T phase diagram shown in Fig. 2(b) indicate the bias points for which LTSLM data are shown. LTSLM voltage images 1–8 in Fig. 2(d) show the evolution of the superconducting properties of the Pb/BFO bridge upon cooling through T_c (from left to right) at $H_{\rm ext} = 0$;

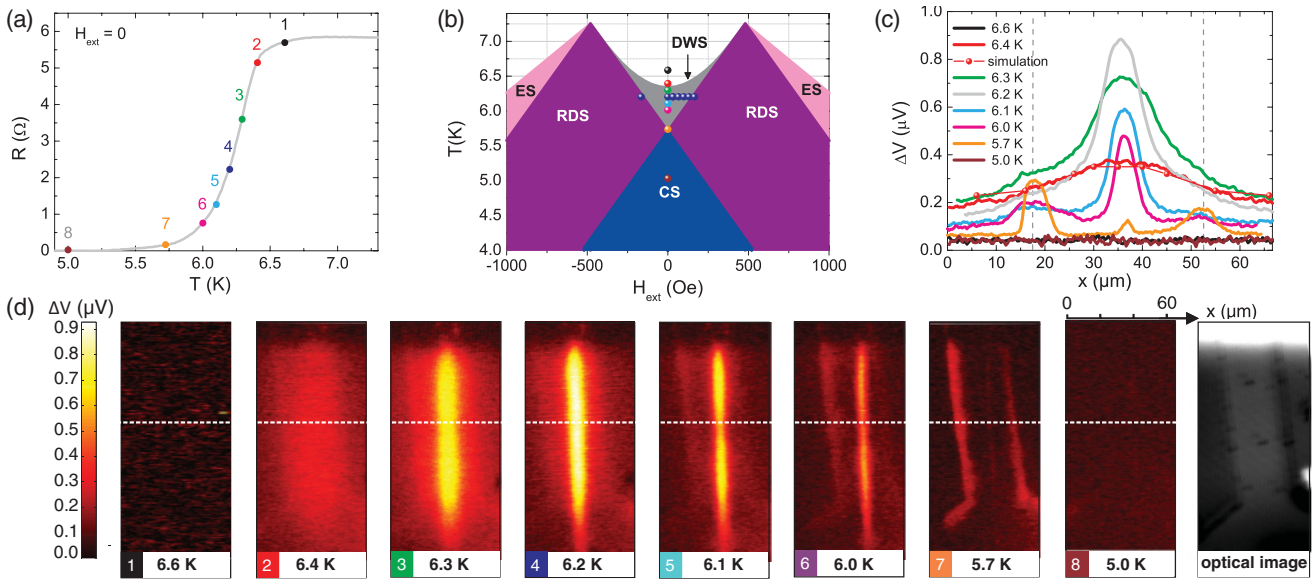

FIG. 2. (Color) Evolution of DWS upon cooling through T_c and $H_{\rm ext}$-T phase diagram. (a) $R(T)$ curve ($I = 100$ μA); dots indicate bias points of LTSLM voltage images 1–8 in (d) and corresponding line scans in (c). (b) $H_{\rm ext}$-T phase diagram, constructed from experimentally determined values $T_{c0} = 7.25$ K, $B_0 = 480$ G, and $H_{c2}^{(0)} = 2.25$ kOe. The phase diagram contains separate regions of DWS, ES, RDS, and CS. Dots label bias points for LTSLM data shown in (c), (d), and Fig. 3. (c) Line scans $\Delta V(x)$ across the bridge for different T, taken from voltage images in (d). Red dots show simulation results for $T = 6.4$ K. The position of the edges of the bridge is indicated by dashed gray lines. (d) Series of LTSLM voltage images $\Delta V(x,y)$ (1–8 from left to right) taken at different T during cooling the Pb bridge through its resistive transition ($I = 10$ μA). White dashed lines indicate the position of line scans in (c). The graph on the right shows a corresponding optical LTSLM image.

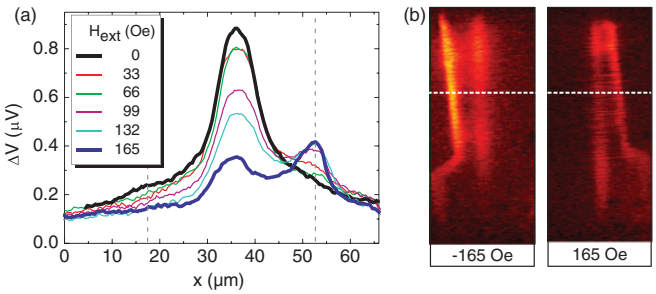

FIG. 3. (Color online) Switching from DWS to RDS: variable H_{ext} at $T = 6.2$ K. (a) Line scans $\Delta V(x)$ along white dashed line in (b) for different $H_{\text{ext}} \gtrless 0$; dashed gray lines indicate edges of the bridge. (b) LTSLM images for maximal $|H_{\text{ext}}|$.

according to Fig. 2(b), these should cover the transitions from the normal state to DWS and finally to CS. The graph on the right shows an optical LTSLM image, in order to indicate size and position of the bridge in the voltage images.[27] For a more quantitative analysis, in Fig. 2(c) we show line scans $\Delta V(x)$ across the bridge [along the white dashed lines in Fig. 2(d)].

Starting with the highest temperature $T = 6.6$ K, the voltage image in Fig. 2(d) and the corresponding line scan (black line) in Fig. 2(c) shows no signal, as the bridge is in the normal state. Lowering T to 6.4 K [entering the resistive transition shown in Fig. 2(a)], the voltage image gives a small homogeneous signal with a broad maximum centered above the bridge [red line in Fig. 2(c)]. For a (still) resistive Pb bridge with homogeneous conductivity but finite $\partial R/\partial T$, this behavior can be simply explained by the finite width of the beam-induced $\delta T(x,y)$ profile, i.e., its tails will induce a voltage signal, even if the beam spot is positioned outside the bridge. This is confirmed by numerical simulations [cf. red data points in Fig. 2(c)], which solve the heat diffusion equation for an absorbed laser power of 25 μW, a beam spot diameter of 2 μm and thermal conductivity of the BFO substrate of 0.8 W cm^{-1} K^{-1}. These simulations yield a maximum increase in beam-induced temperature $\Delta T = 0.14$ K.

Upon further cooling (see voltage images and corresponding line scans for $T = 6.3$ K and $T = 6.2$ K), a clear LTSLM signal develops, running along the domain wall [green and blue lines, respectively, in Fig. 2(c)]. This observation can be interpreted as an evidence that a channel above the domain wall with higher conductivity than the regions above the domains has formed, and therefore the current density $j(x)$ has a maximum above the domain wall. We note that, although according to the H_{ext}-T phase diagram the sample should be in the the DWS state, the overall resistance of the bridge is close to the full normal resistance. This is consistent with numerical simulations based on the time-dependent Ginzburg-Landau equations, which indicate that for our experimental situation the critical current density $j_{c,\text{DWS}}$ along the domain-wall channel is too small, i.e., the bias current might be above the critical current of this channel. This also explains why, upon decreasing T, the LTSLM signal at the domain wall increases, as $j_{c,\text{DWS}}$ increases, and the peak in $\Delta V(x)$ becomes sharper (see below). We did not find a similar enhancement of the LTSLM voltage signal at the edges of the bridge, i.e., we do not find any signature of ES. We attribute this to the finite width of the domain wall, which stabilizes DWS compared to ES.

For $T < 6.2$ K the amplitude of the peak of the LTSLM response at the domain wall decreases as T decreases, and the maximum of the LTSLM signal shifts toward the edges of the bridge; see magenta and orange lines in Fig. 2(c) for $T = 6.0$ K and $T = 5.7$ K, respectively, and the corresponding voltage images in Fig. 2(d). We interpret this observation as the transition from DWS to CS, which is consistent with the phase diagram shown in Fig. 2(b). At this transition, CS spreading over the whole sample becomes favorable and the sample is turned into the mixed state. The onset of CS can explain the appearance of two pronounced maxima in $\Delta V(x)$ at the sample edges: In the mixed state the current distribution depends on the edge energy barrier for vortex entry. Upon laser irradiation, the edge energy barrier is locally suppressed, which in turn opens a gate for vortex entry/exit. Hence one can expect that irradiation at the edges of the bridge should strongly affect the vortex pattern and the resulting current distribution. In contrast, laser irradiation of the interior of the bridge does not change the existing energy barrier, and the modification of the current pattern is probably less pronounced, and therefore the beam-induced voltage change is much smaller. Finally, at $T = 5.0$ K the LTSLM signal is zero [cf. Fig. 2(d) and brown line in Fig. 2(c)], which indicates that the bridge is in the CS state and the beam-induced perturbation is not strong enough to suppress superconductivity and induce a voltage signal.

Finally, we investigated the effect of finite perpendicular field $|H_{\text{ext}}| \leqslant 165$ Oe on superconductivity in our system. The measurements were carried out at $T = 6.2$ K, which corresponds to the most pronounced LTSLM signal above the domain wall at $H_{\text{ext}} = 0$. Figure 3(a) shows the evolution of the LTSLM voltage signal $\Delta V(x)$ with increasing external field for positive polarity. For $H_{\text{ext}} = 0$ the DWS signal is clearly visible as described above. With increasing H_{ext} the amplitude of the domain-wall signal decreases monotonously while its width stays roughly constant. Simultaneously a signal above the reverse (right) domain appears. In the RDS state, for $H_{\text{ext}} \gtrsim 70$ Oe, the voltage signal shows a peak at the right edge of the bridge, which can be explained in the same way as for the edge signal discussed in the context of the T series shown in Fig. 2. Figure 3(b) shows LTSLM voltage images taken at $H_{\text{ext}} = -165$ Oe (left image) and $H_{\text{ext}} = +165$ Oe (right image), which clearly demonstrate switching between the RDS states above the two domains upon reversing the polarity of the external field.

In conclusion, we have clearly identified the formation of the spatially inhomogeneous superconducting state in a superconducting Pb thin film induced by the stray field of the domains in the ferromagnetic substrate BFO underneath. The crucial feature of the investigated system is that the superconducting Pb bridge was fabricated exactly above a single straight domain wall, which is running along the center of the bridge. Such a well-defined geometry of the hybrid Pb/BFO sample makes it possible to directly visualize the localized and delocalized superconductivity by means of low-temperature scanning laser microscopy. We imaged the evolution of DWS with decreasing temperature. Using the external field as a control parameter, we demonstrated that superconductivity in

a wide superconducting bridge can be switched from the DWS to RDS state. This opens up interesting perspectives for the creation of spatially nonuniform superconducting states and for their manipulation by external and "internal" magnetic fields.

This work was funded by DFG via Grant No. KO 1303/8-1, the Methusalem Funding of the Flemish Government, the NES-ESF program, the Belgian IAP, the Fund for Scientific Research–Flanders (F.W.O.-Vlaanderen), the RFBR, RAS under the Program "Quantum physics of condensed matter," and FTP "Scientific and educational personnel of innovative Russia in 2009–2013." R.W. gratefully acknowledges support by the Cusanuswerk, Bischöfliche Studienförderung.

*koelle@uni-tuebingen.de

[1] I. Tamm, Phys. Z. Sowjetunion **1**, 733 (1932).

[2] W. Shockley, Phys. Rev. **56**, 317 (1939).

[3] R. H. Ritchie, Phys. Rev. **106**, 874 (1957).

[4] L. D. Landau and E. M. Lifshitz, *Electrodynamics of Continuous Media*, 2nd ed. (Pergamon, New York, 1984).

[5] S. A. Maier, *Plasmonics: Fundamentals and Applications* (Springer, New York, 2007).

[6] Lord Rayleigh, in Proc. London Math. Soc. **17**, 4 (1885).

[7] *Acoustic Surface Waves*, Topics in Applied Physics Vol. 24, edited by A. A. Oliner (Springer-Verlag, Berlin, 1978).

[8] D. Saint-James and P. G. de Gennes, Phys. Lett. **7**, 306 (1963).

[9] D. Saint-James, G. Sarma, and E. J. Thomas, *Type II Superconductivity* (Pergamon, New York, 1969).

[10] R. H. White, Phys. Rev. **142**, 241 (1966).

[11] A. Y. Aladyshkin, D. A. Ryzhov, A. V. Samokhvalov, D. A. Savinov, A. S. Melnikov, and V. V. Moshchalkov, Phys. Rev. B **75**, 184519 (2007).

[12] M. Tinkham, *Introduction to Superconductivity*, 2nd ed. (McGraw-Hill, New York, 1996).

[13] A. Y. Aladyshkin, A. V. Silhanek, W. Gillijns, and V. V. Moshchalkov, Supercond. Sci. Technol. **22**, 053001 (2009).

[14] A. I. Buzdin and A. S. Mel'nikov, Phys. Rev. B **67**, 020503(R) (2003).

[15] A. Y. Aladyshkin, A. I. Buzdin, A. A. Fraerman, A. S. Mel'nikov, D. A. Ryzhov, and A. V. Sokolov, Phys. Rev. B **68**, 184508 (2003).

[16] We calculate $|\Psi(x)|$ by solving numerically the linearized Ginzburg-Landau equation for a thin superconducting bridge of finite width in the presence of the nonuniform field $B_z(x) = H_{\rm ext} + (2B_0/\pi)\arctan(x/L)$, following the approach of Ref. 15. The case $L \to 0$ corresponds to a steplike field profile, and any (even very small but) finite L gives a finite transient region for the stray magnetic field near the domain wall. I.e., for the system investigated here, with typical width 5–10 nm of the domain walls in the $BaFe_{12}O_{19}$ substrate, ES will be suppressed.

[17] Z. R. Yang, M. Lange, A. Volodin, R. Szymczak, and V. V. Moshchalkov, Nat. Mater. **3**, 793 (2004).

[18] J. Fritzsche, V. V. Moshchalkov, H. Eitel, D. Koelle, R. Kleiner, and R. Szymczak, Phys. Rev. Lett. **96**, 247003 (2006).

[19] A. Y. Aladyshkin, A. P. Volodin, and V. V. Moshchalkov, J. Appl. Phys. **108**, 033911 (2010).

[20] J. Fritzsche, R. B. G. Kramer, and V. V. Moshchalkov, Phys. Rev. B **80**, 094514 (2009).

[21] A. Y. Aladyshkin, J. Fritzsche, and V. V. Moshchalkov, Appl. Phys. Lett. **94**, 222503 (2009).

[22] A. P. Zhuravel, A. G. Sivakov, O. G. Turutanov, A. N. Omelyanchouk, S. M. Anlage, A. Lukashenko, A. V. Ustinov, and D. Abraimov, Low Temp. Phys. **32**, 592 (2006).

[23] A. Lukashenko, A. V. Ustinov, A. P. Zhuravel, E. Hollmann, and R. Wördenweber, J. Appl. Phys. **100**, 023913 (2006).

[24] M. Wagenknecht, H. Eitel, T. Nachtrab, J. B. Philipp, R. Gross, R. Kleiner, and D. Koelle, Phys. Rev. Lett. **96**, 047203 (2006).

[25] H. B. Wang, S. Guénon, J. Yuan, A. Iishi, S. Arisawa, T. Hatano, T. Yamashita, D. Koelle, and R. Kleiner, Phys. Rev. Lett. **102**, 017006 (2009).

[26] A. Yu. Aladyshkin, J. Fritzsche, R. Werner, R. B. G. Kramer, S. Guenon, R. Kleiner, D. Koelle, and V. V. Moshchalkov, e-print arXiv:1105.1596 (to be published).

[27] The bright area in the upper part of the optical image is due to an Au contact layer on top of the Pb film, which gives a strongly enhanced reflected laser signal and due to reduced absorbtion a reduction of the LTSLM signal, which can be clearly seen in images 2–7 in Fig. 2(d).